Sirt1 mediates neuroprotection from mutant huntingtin by activation of TORC1 and CREB transcriptional pathway

Hyunkyung Jeong[1*], Dena E. Cohen[2*], Libin Cui[1], Andrea Supinski[2], Jeffrey N. Savas[3], Joseph R. Mazzulli[1], John R. Yates[3]. Laura Bordone[4], Leonard P. Guarente[2+], and Dimitri Krainc[1+]

Supplementary Information

Supplementary Figure 1

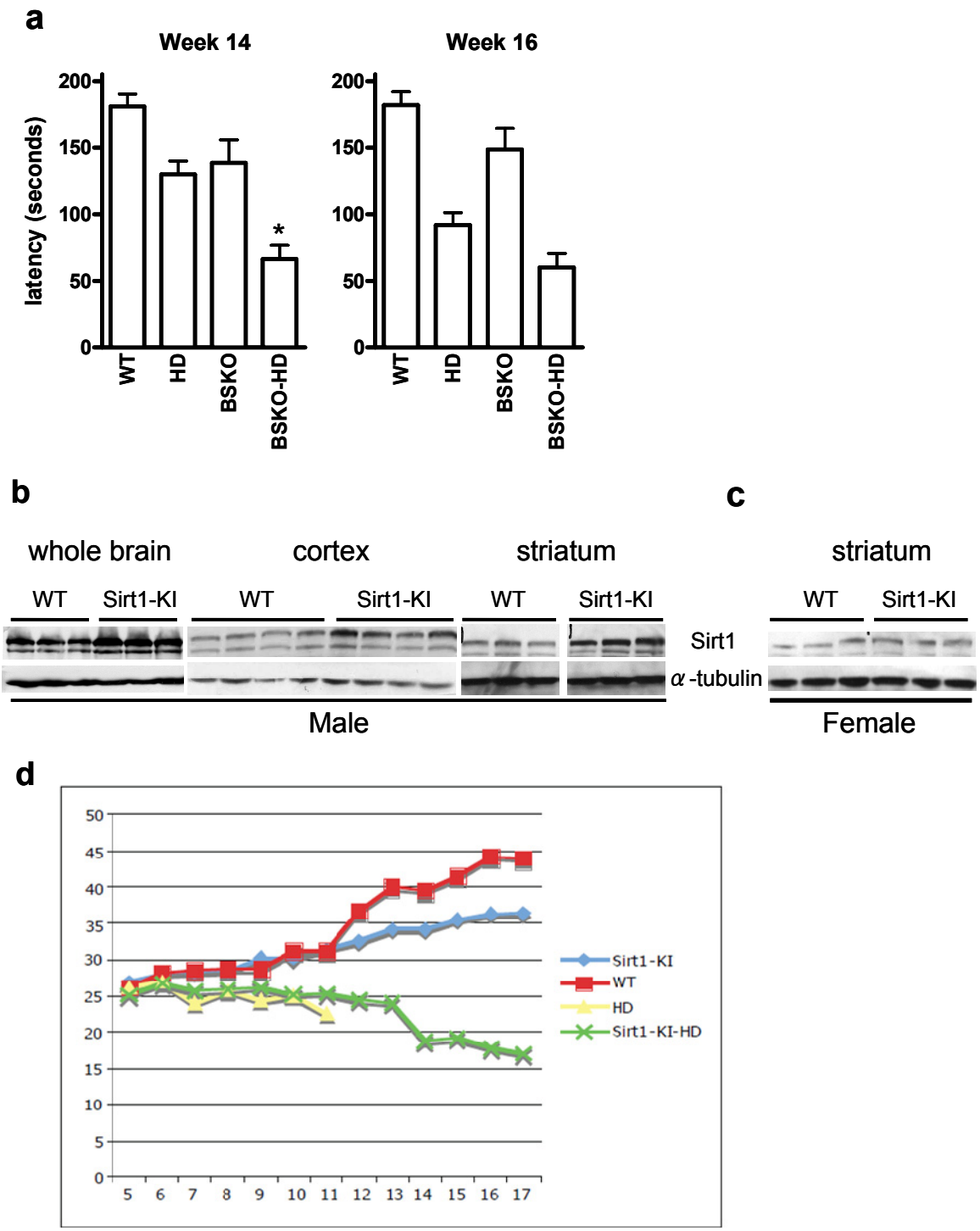

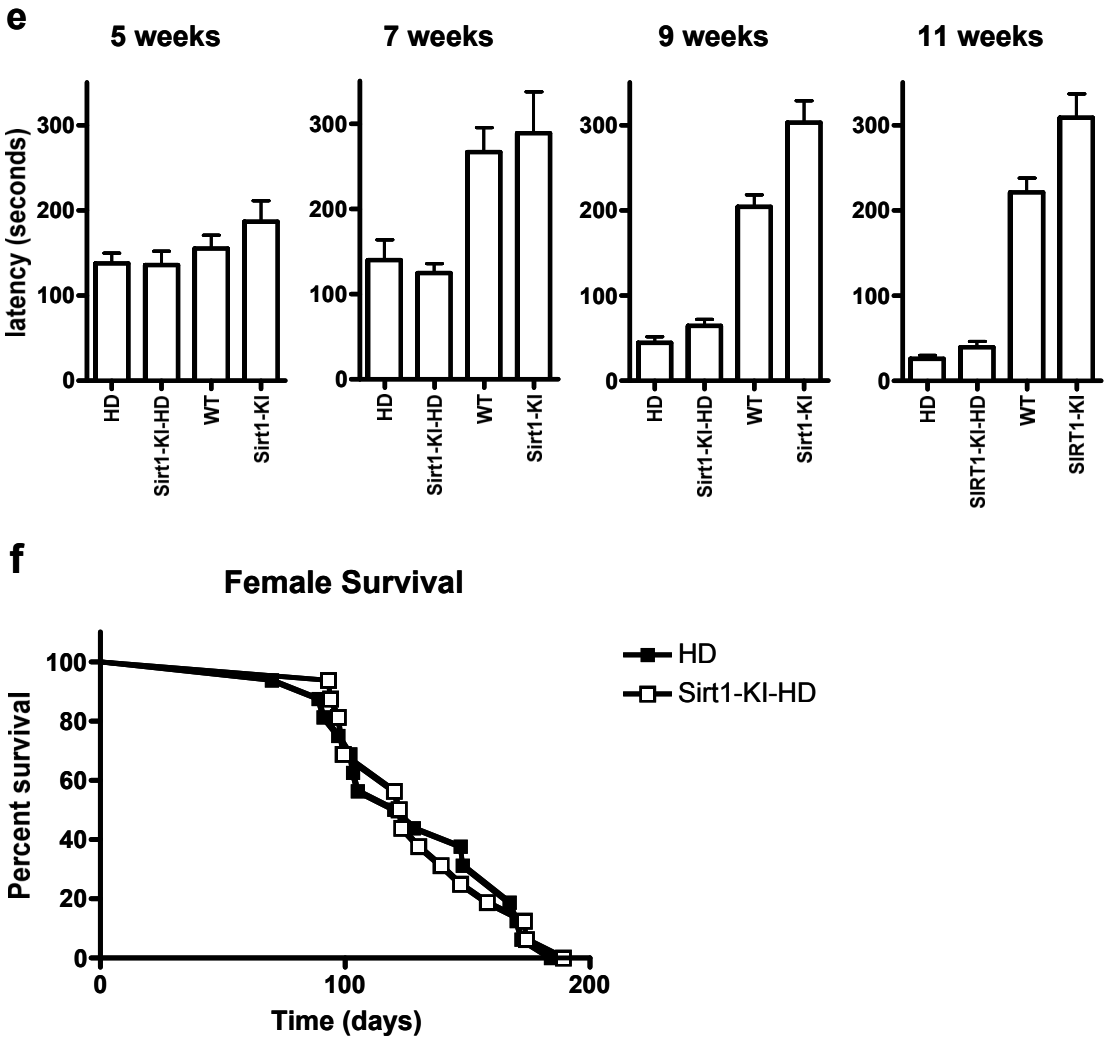
e
5 weeks
7 weeks
9 weeks
11 weeks
latency (seconds)
0
100
200
300
HD
Sirt1-KI-HD
WT
Sirt1-KI
SIRT1-KI-HD
SIRT1-KI
f
Female Survival
Percent survival
0
20
40
60
80
100
0
100
200
Time (days)
HD
Sirt1-KI-HD

Supplementary Figure 1. The effects of Sirt1 deletion or overexpression on R6/2 mice. **a**. Deletion of Sirt1 worsens behavioral phenotype of R6/2 mice. An accelerating rota-rod assay was used to assess the motor coordination of mice of the indicated genotypes and ages. The amount of time that each mouse was able to remain on the rotating rod was recorded for four trials per animal per time point. $n = 4–10$ animals per group. $*P < 0.05$ for R6/2 vs. BSKO-R6/2 by ANOVA. **b**. Sirt1-KI mice over-express Sirt1 in brain. Expression of Sirt1 protein was analyzed in extracts prepared from whole brain, cortex, or striatum dissected from 3 month old male mice of the indicated genotypes. α-tubulin was analyzed as a loading control. **c**. Lower degree of Sirt1 expression was observed in striata of female Sirt1-KI mice. α-tubulin was analyzed as a loading control. **d**. Sirt1 over-expression does not affect body weight loss in HD mice. Mice were weighed weekly beginning at 5 weeks of age, and their weight in grams recorded. No significant differences were observed between the weight of HD mice and Sirt1-KI mice at any age. Sirt1-KI mice were lighter than WT mice at later ages, as had been reported previously[1]. **e**. Sirt1 over-expression does not improve motor performance in HD mice. An accelerating rotarod assay was used to assess the motor phenotype of male mice of the indicated genotypes and ages. No statistically significant differences were observed between HD and Sirt1-KI-HD mice at any age. A statistically significant difference between WT and Sirt1-KI mice was observed at 11 weeks ($P < 0.05$, ANOVA), consistent with the previously reported phenotype of these animals[1]. **f**. Sirt1 over-expression does not extend lifespan in female R6/2 mice. The lifespan of female HD and Sirt1-HD mice was determined and plotted ($n = 13–15$ per group). No differences in survival were detected.

Supplementary Figure 2

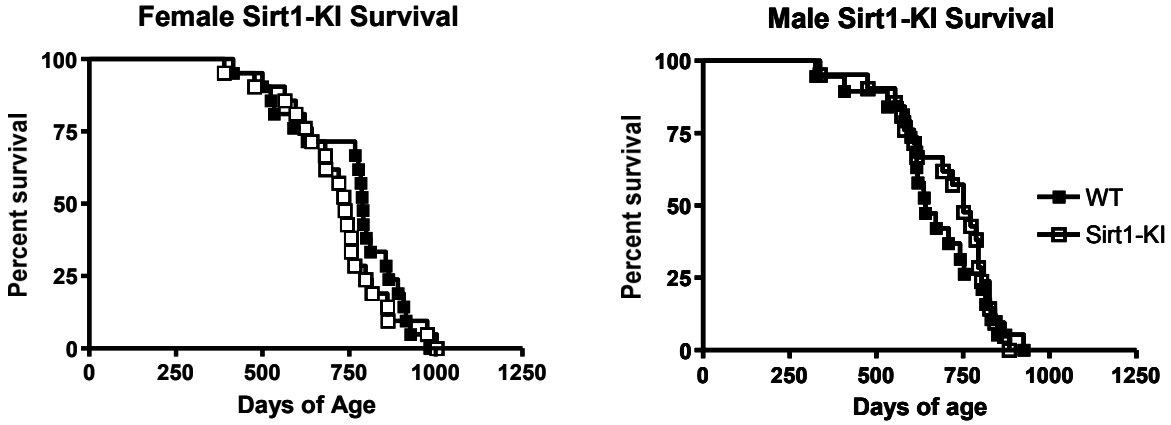

Supplementary Figure 2. Sirt1-KI does not extend lifespan. Sirt1-KI mice and their WT littermates on an outbred background were analyzed to determine whether the Sirt1-KI allele extended lifespan. Males and females were analyzed separately. No statistically significant differences in lifespan were detected for either gender (n = 25–30 per group).

Supplementary Figure 3

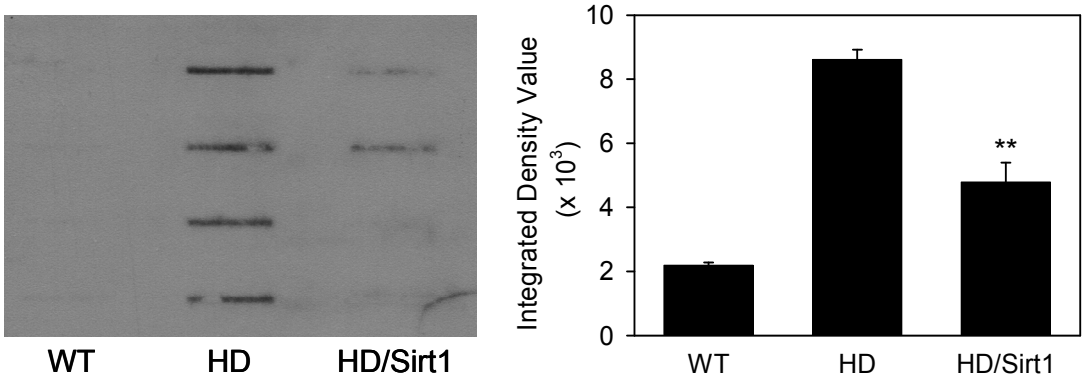

Supplementary Figure 3. Decreased aggregation was detected in R6/2 mice (HD) crossed with Sirt1-KI mice (Sirt1) compared to R6/2 mice. Filter trap assay of SDS-resistant insoluble aggregates from brain tissues of male WT, R6/2 (HD) and HD/Sirt1 mice. The filter membrane was probed with EM48 anti-*HTT* antibody. $^{**}P < 0.001$ vs HD.

Supplementary Figure 4

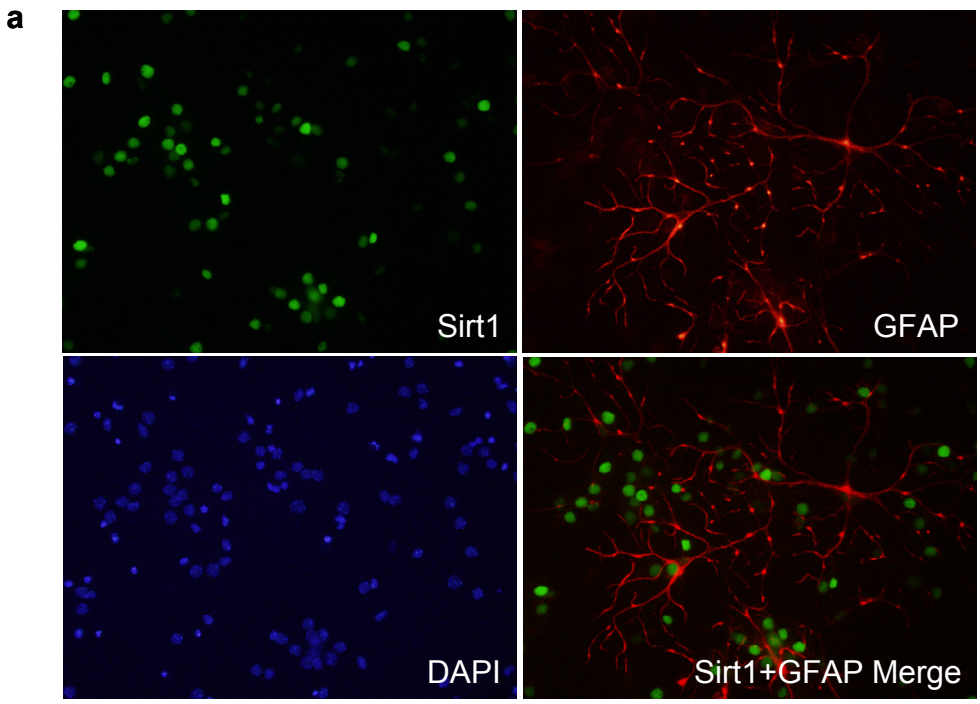

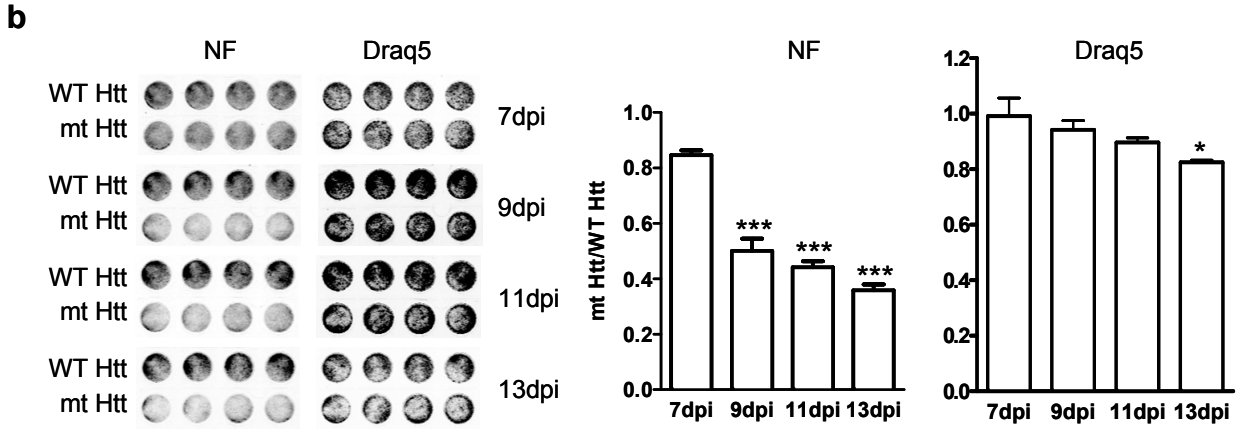

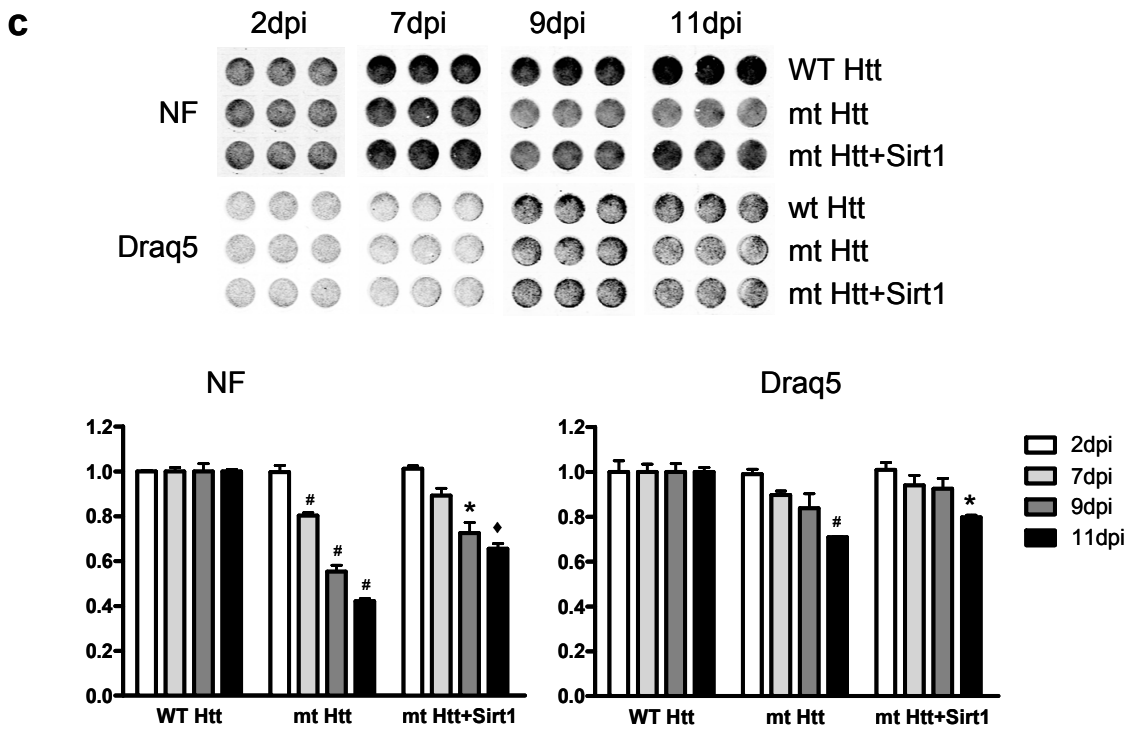

Supplementary Figure 4. Characterization of lentivirally-mediated expression of mutant *HTT* in primary neurons. **a**. Lentiviral expression of Sirt1 driven by PGK promoter is neuron-specific. Mouse cortical neurons were stained for Sirt1 (green), glial marker GFAP (red) and DAPI (blue). GFAP-expressing cells that were rarely found in these cultures did not express lentiviral Sirt1. Representative images are shown. **b**. Time-dependent toxicity in primary neurons expressing mutant *HTT*. Rat primary cortical neurons were infected on DIV4 with lenti WT or mutant *HTT* as in **fig. 2a**, **b** and double stained with antibody to neurofilament (NF) (left panels) and Draq5 to examine the nuclei (right panel) on indicated days post infection (dpi). Quantification of the ratio of NF or Draq5 staining intensity of mutant *HTT*-expressing neurons vs. WT *HTT*-expressing neurons was performed on indicated days post infection. ***$P < 0.001$ vs 7dpi. *$P < 0.05$ vs 7dpi. **c**. Loss of neurites precedes nuclear toxicity in mutant *HTT*-expressing primary neurons. In cell western was performed to measure NF staining intensity and nuclear staining intensity (draq5) in mouse primary cortical neurons transduced with WT *HTT*, mutant *HTT* or mutant *HTT* and Sirt1 lentivirus. Overexpression of Sirt1 rescues both NF and nuclear toxicity of mutant *HTT*. #$P < 0.001$ vs wt *HTT*, *$P < 0.05$ vs mt *HTT*, ♦$P < 0.001$ vs mt *HTT*.

Supplementary Figure 5

NAME	SIZE	ES	NES	NOM p-val	FDR q-val
AXON GUIDANCE	21	-0.68801284	-2.0317764	0	0.0293116
NEURITE DEVELOPMENT	52	-0.5021753	-1.8506379	0.0032	0.1837541
CELLULAR MORPHOGENESIS DURING DIFFERENTIATION	47	-0.50466734	-1.8149486	0.00506757	0.1867073
AXONOGENESIS	42	-0.53403777	-1.8673615	0	0.2023901
NEURON DIFFERENTIATION	75	-0.4344133	-1.6828823	0.00474684	0.2554342
NEURON DEVELOPMENT	60	-0.47509512	-1.7592392	0.0046875	0.260192

Supplementary Figure 5. GSEA (Gene Set Enrichment analysis)[2] of striatal gene expression shows rescue of neurite development and differentiation pathways in Sirt1-KI-R6/2 compared to R6/2 mice.

Supplementary Figure 6

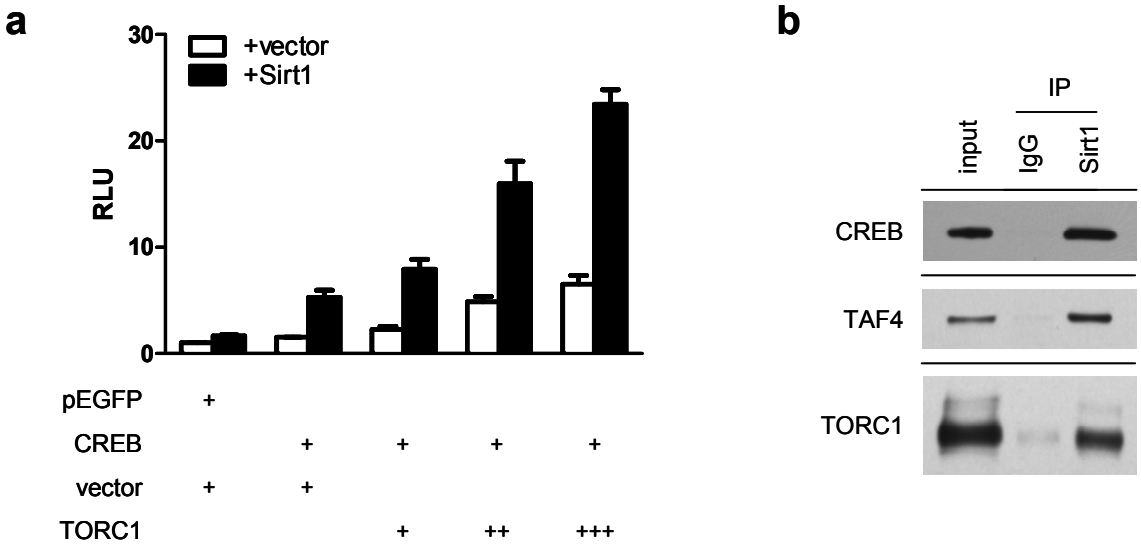

Supplementary Figure 6. Sirt1 interacts with CREB and TORC1 and potentiates their transcriptional activity. **a**. Potentiation of CREB-TORC1-mediated activation of BDNF transcription by Sirt1. BDNF reporter activity was measured in N2a cells transfected with BDNF IV Promoter-luciferase (pIII(170)Luc) together with indicated plasmids and luciferase activity measured at 24 hr post transfection. White bars represent vector cotransfection and black bars represent Sirt1 cotransfection. Three independent experiments were done. **b**. Sirt1 interacts with CREB, TAF4 and TORC1. N2a cells were transfected with Myc-Sirt1 and Flag-CREB, HA-TAF4 or TORC1. Co-immunoprecipitation assay was performed with antibody to Myc and probed for Flag-CREB, HA-TAF4 or TORC1. IgG was used in place of antibody to Myc to assess for nonspecific binding to protein G beads.

Supplementary Figure 7

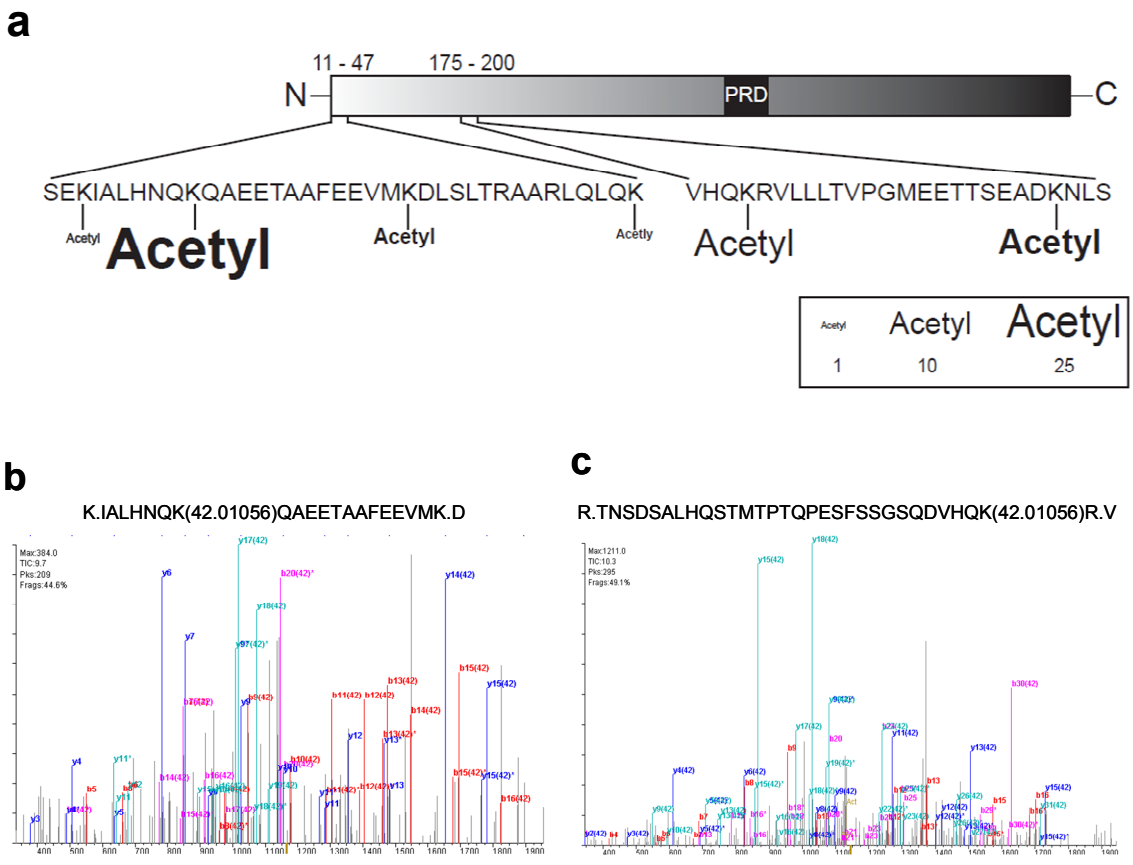

Supplementary Figure 7. TORC1 is acetylated at multiple lysines (K13, K20, K33, K47, K178, K197). **a**. Human TORC1 protein schematic with lysine acetylation sites as identified by high resolution mass spectrometry. Acetylation sties identified in multiple analyses are shown in bold and the font size represents the quantity of MS spectra where each site was identified and localized. **b** and **c**. Representative LC-MS/MS spectra of the acetylated peptides from human TORC1. The unfragmented peptide as well as a series of b and y-ions displayed a mass change of +42 Da, indicative of acetylation. Fragment ions detected with +42Da are annotated as (42).
b. K20; K.IALHNQK(42.01056)QAEETAAFEEVMK.D,
c. K178; R.TNSDSALHQSTMTPTQPESFSSGSQDVHQK(42.01056)R.V

Supplementary Figure 8

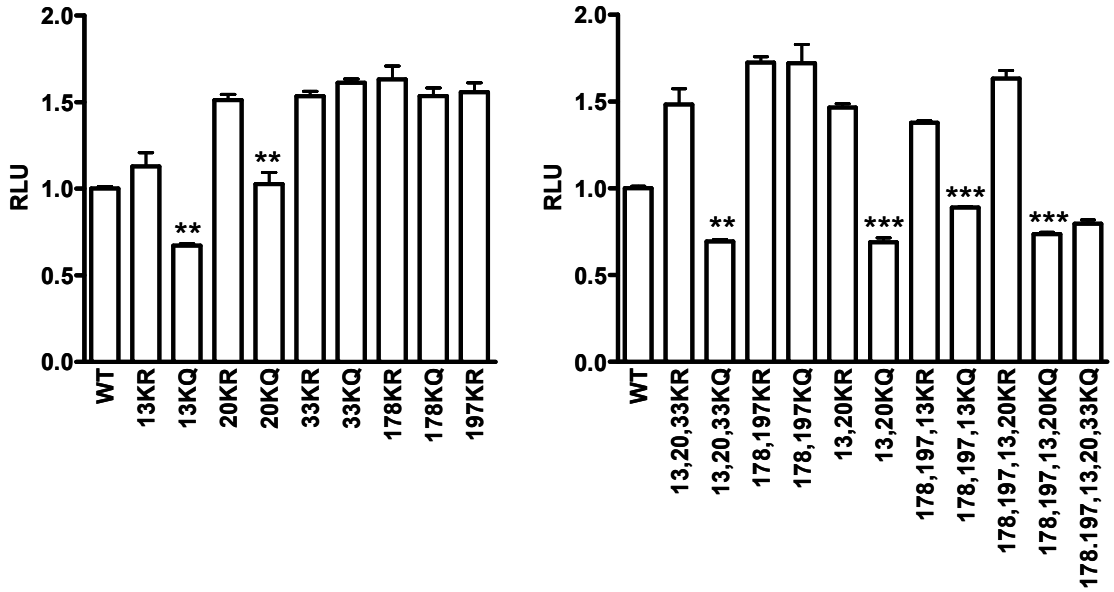

Supplementary Figure 8. Deacetylation of lysines 13 and 20 in TORC1 protein promotes activation of BDNF promoter IV. Activation of BDNF promoter IV was assessed in Neuro2a cells were transfected with pIII170 luc together with CREB and indicated TORC1 mutants and luciferase activity measured at 24 h posttransfection. Expression levels of transfected constructs were carefully monitored to ensure equal expression. $^{**}P < 0.01$ vs KR, $^{***}P < 0.001$ vs KR.

Supplementary Figure 9

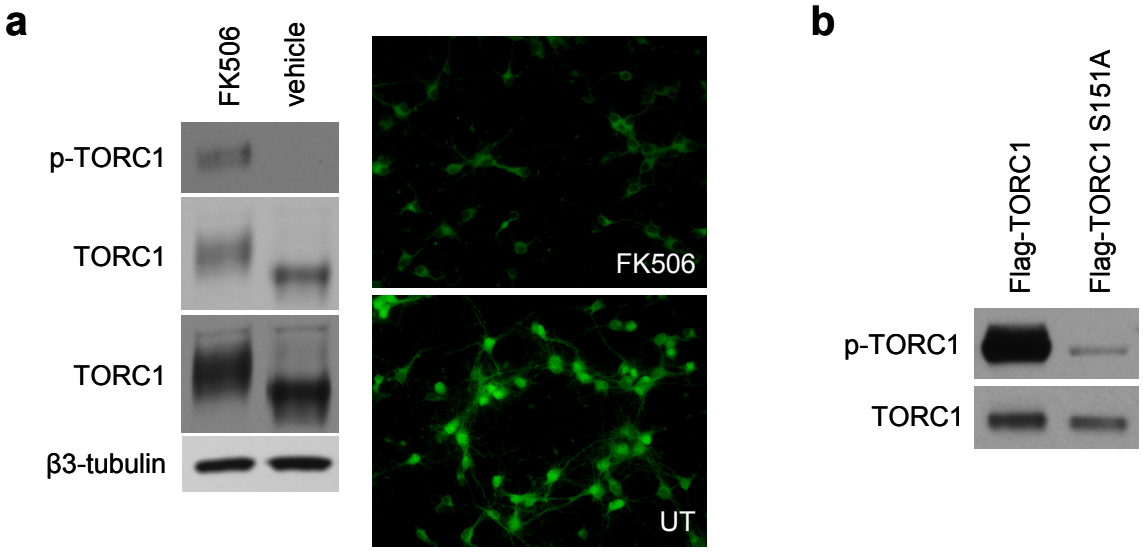

Supplementary Figure 9. Characterization of TORC1 phosphorylation in primary neurons. **a**. Faster-migrating forms of TORC1 represent nuclear TORC1 that is dephosphorylated at S151. Calcineurin inhibitor FK506 increases phospho TORC1 which corresponds to cytoplasmic, slower-migrating form. Two different exposures are shown for total TORC1 (middle two panels). Primary cortical neurons were treated with vehicle (UT) or 5 μM FK506 for 6 h at DIV5 and endogenous TORC1 detected with antibody to TORC1. β3-tubulin was used as loading control. **b**. Characterization of phospho S151 TORC1 antibody. Mutation of Ser151 to Ala shows reduced reactivity to phospho S151 TORC1 antibody (upper panel). The protein levels of total TORC1 are shown in lower panel.

Supplementary Figure 10

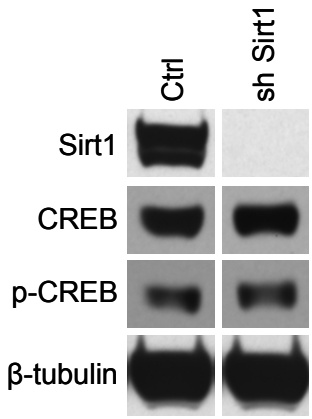

Supplementary Figure 10. Knockdown of Sirt1 in primary cortical neurons does not affect levels of total CREB and phospho CREB. Preparations and lentiviral infections of primary cortical neurons were done as described in **fig. 3g**.

Supplementary Figure 11

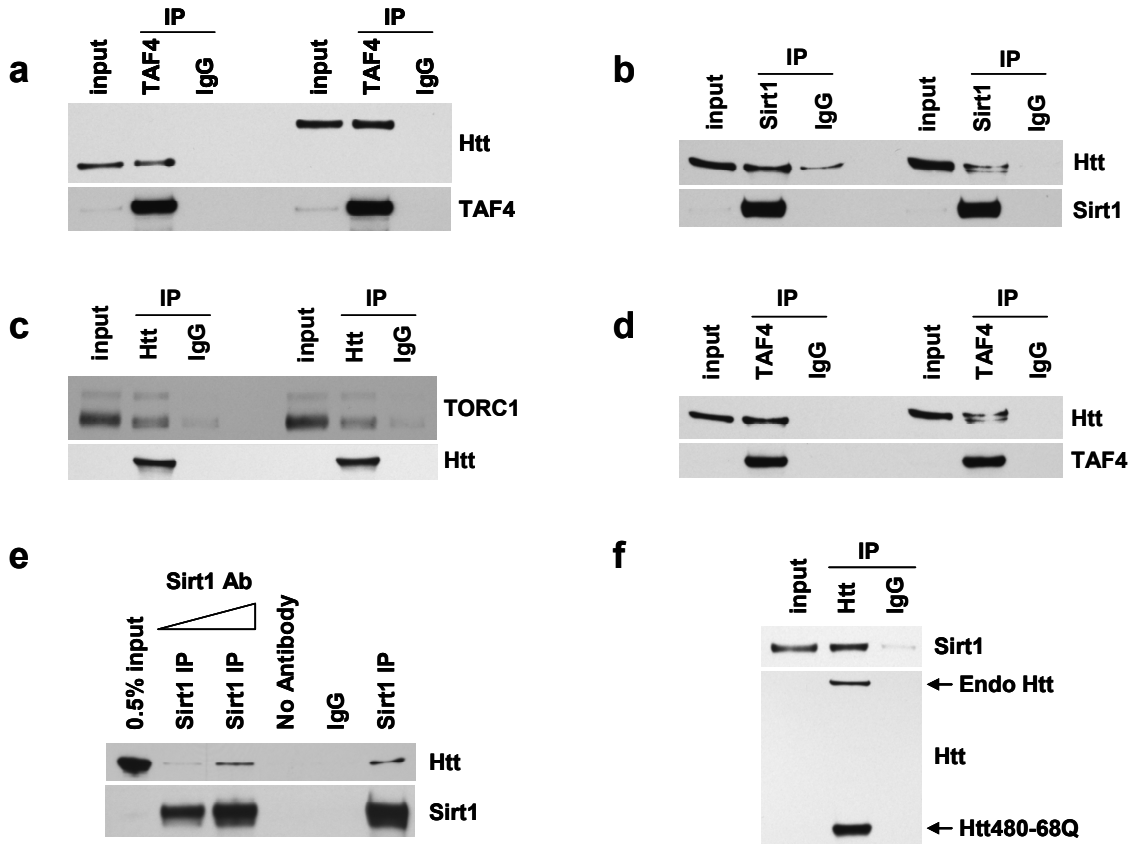

Supplementary Figure 11. WT and mutant *HTT* interact with TAF4, TORC1 and Sirt1. Neuro2a cells were transfected with *HTT*480-17Q or *HTT*480-68Q and HA-TAF4 (**a**), with full-length WT *HTT* (HD17) or full-length mutant *HTT* (HD75) and Myc-Sirt1 (**b**), with HD17 or HD75 and TORC1 (**c**) or with HD17 or HD75 and HA-TAF4 (**d**). Coimmunoprecipitation was performed at 24 h posttransfection with antibody to HA (TAF4) (**a** and **d**), with antibody to Myc (Sirt1) (**b**) or with antibody to *HTT* (MAB2166) (**c**). Coimmunoprecipitating proteins were detected by probing membranes with antibody to *HTT* (MAB 2166, **a**, **b** and **d**) or antibody to TORC1 (**c**). **e.** Endogenous Sirt1 interacts with endogenous full-length WT *HTT* in Neuro2a cells. Increasing amounts of Sirt1 antibody were used for IP of endogenous Sirt1. IgG and no antibody IP were used as negative controls. **f.** Mutant *HTT* fragment (*HTT*480-68Q) interacts with endogenous Sirt1 in Neuro2a cells. Coimmunoprecipitation was performed at 24 h after transfection of *HTT*480-68Q. Top panel shows coimmunoprecipitating endogenous Sirt1. IgG IP was used as negative control. A modest degree of over expression of mutant *HTT* (*HTT*480-68Q) is shown in comparison to endogenous full-length WT *HTT* (endo *HTT*).

Supplementary Figure 12

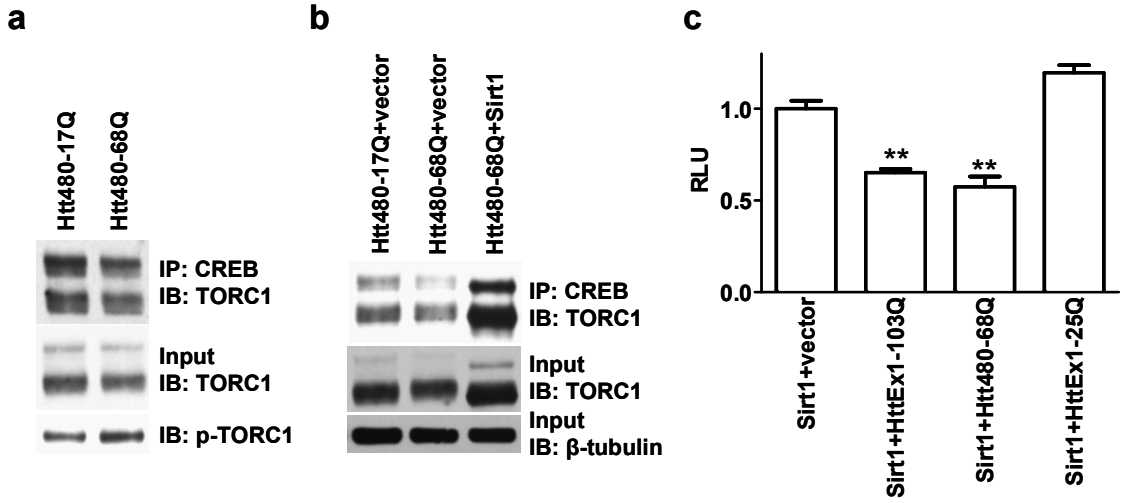

Supplementary Figure 12. Mutant huntingtin interferes with CREB-TORC1 interaction and Sirt1 transcriptional activity. **a.** Mutant *HTT* disrupts CREB-TORC1 interaction. Neuro2a cells were transfected with Flag-CREB, TORC1, *HTT*480-17Q or *HTT*480-68Q, immunoprecipitated with anti-Flag antibody and probed with anti-TORC1 antibody (top panel). Input samples were probed with antibody to TORC1 (middle panel) and antibody to phospho-TORC1 (bottom panel), respectively. **b.** Sirt1 rescues mutant *HTT*-mediated disruption of CREB-TORC1 interaction. Neuro2a cells were transfected as above together with vector or Sirt1, immunoprecipitated with antibody to Flag and probed with antibody to TORC1. β-tubulin was used as loading control. **c**. Mutant *HTT* inhibits Sirt1-mediated activation of BDNF reporter. N2a cells were transfected with pIII(170)Luc BDNF promoter-reporter, Sirt1 and vector, mutant *HTT* or WT *HTT*. Luciferase activity assay was performed at 48 h posttransfection. $^{**}P < 0.01$ vs. Sirt1 + vector. Four independent experiments were done.

Supplementary Figure 13

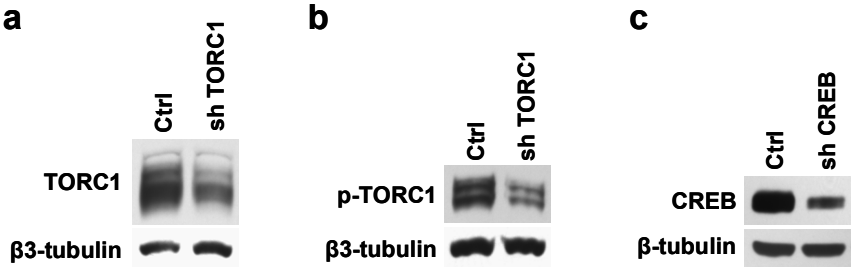

Supplementary Figure 13. Knockdown of TORC1, phospho TORC1 and CREB in primary neurons infected with control or sh TORC1 or sh CREB lentivirus as shown by western blotting. Lenti-control, lenti-sh TORC1 or lenti-sh CREB were infected at DIV7 mouse cortical neurons at moi of 2, and samples analyzed at 5 days post infection. β3-tubulin or β-tubulin was used as loading control.

Supplementary Figure 14

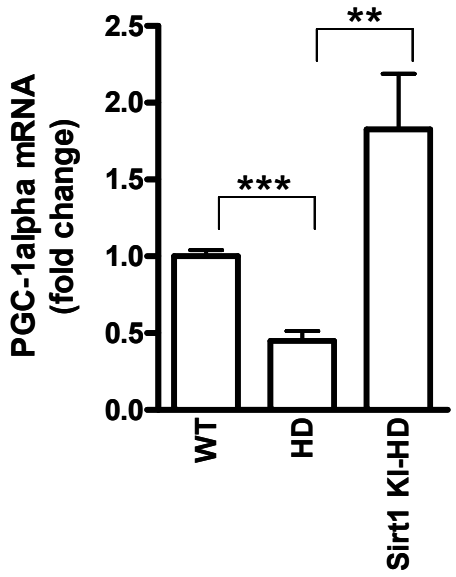

Supplementary Figure 14. Over-expression of Sirt1 restores PGC-1alpha expression in brains of R6/2 mice. PGC-1alpha mRNA levels in the forebrain of mice of the indicated genotypes were measured by qRT-PCR at 12 weeks of age. Total RNA was prepared using RNeasy Lipid Tissue Mini Kit (Qiagen). First strand cDNA and realtime qPCR were performed using SuperScript III First-Strand Synthesis SuperMix (Invitrogen), QuantiFast SYBR Green PCR Kit (Qiagen) and an Eppendorf Mastercycler. The real-time PCR primers for mouse PGC-1alpha mRNA and control 18S rRNA are as follow: PGC-1alpha Forward 5'-GTAGGCCCAGGTACGACAGC-3' and PGC-1 alpha Reverse 5'-GCTCTTTGCGGTATTCATCCC-3'; 18S rRNA Forward 5'-AAACGGCTACCACATCCAAG-3' and 18S Reverse 5'-CCTCCAATGGATCCTCGTTA-3'. PGC-1 alpha mRNA levels were calculated according to DDCt method with WT group used as control. Data are means of fold changes ± SEM, $n = 4$ animals in each group. ***$P < 0.001$, **$P < 0.01$ by t-test.

Supplementary Methods

Full Methods

Mouse Studies. To generate BSKO-R6/2 mice, *Sirt1*$^{flox/flox}$-nestin-cre and R6/2 were intercrossed for two generations. Nestin-cre was always passed through the male germline. Because BSKO- R6/2 males bred extremely poorly, we instead crossed *Sirt1*$^{flox/+}$-nestin-cre-R6/2 males with *Sirt1*$^{flox/flox}$ females to obtain the desired experimental groups. These crosses were all carried out on a C57BL/6 background, with an average CAG repeat size of approximately 200. R6/2 mice on the C57BL6/J background were obtained from Psychogenics, Inc. No correlation between Sirt1 or nestin-cre genotype and CAG repeat length was observed. Due to the difficulty in obtaining sufficient numbers of animals, we pooled equal numbers of male and female animals into each group for analysis. Sirt1-KI-R6/2 mice were generated by intercrossing mice heterozygous for the Sirt1-KI transgene, maintained on an outbred background[1] with R6/2 mice on the B6CBAF1/J background (Jackson Laboratories). CAG repeat length was approximately 100–105 repeats, and no correlation between CAG repeat length and Sirt1-KI genotype was observed. Rotarod analysis was performed using a Rotamex-5 Rota Rod apparatus (Columbus Instruments). Mice were trained on the apparatus at the age of 4 weeks using two training sessions of 1 minute each at 4 rpm on consecutive days. Mice were tested at the indicated ages using an accelerating paradigm in which rod speed increased from 4–40 rpm over the course of 600 seconds. Mice remaining on the rod for the entire trial period were assigned a score of 600 seconds. Mice were tested on two consecutive days at each time point, and completed two trials per test day, with a minimum of 30 minutes rest between trials. The four measurements per mouse per time point were averaged to calculate the mouse's score for that time point. For neuropathological analyses, brain sections were examined stereologically as described[3]. Briefly, unbiased estimates of number–weighted mean neuronal volumes were determined using the optical fractionator and nucleator probes (Micro BrightField). Objective used to estimate the volumes of striatal cells was 363; counting frame 50350 mm, sampling grid 1003100 (x and y); average section thickness after histological processing, 7.0 mm (top guard zone, 3 mm, and bottom, 4mm); ANOVA with post hoc t tests was performed to identify significant differences. The dissector counting method was used to assess striatal neurons and *HTT*-positive aggregates using an unbiased random selection of serial sections in a defined volume of the neostriatum, as described[4].

Quantitative PCR. mRNA was isolated from the indicated brain regions using Trizol reagent (Invitrogen). Following treatment with DNase (Promega), RNA was reverse-transcribed using MMLV reverse transcriptase (Invitrogen) and random hexamer primers (New England Biolabs). qPCR was performed using iQ SYBR Green Supermix (Bio-Rad Laboratories) on a Light Cycler 480 II (Roche). Primers used were: BDNF-F: 5'-TCATACTTCGGTTGCATGAAGG-3', BDNF-R: 5'-AGACCTCTCGAACCTGCCC-3' 18S-F: 18S-R: as obtained from the Harvard Primer Bank[5]. Cycling parameters were as

described by the Harvard Primer Bank. Relative mRNA abundance was calculated using the ΔΔCT method.

Plasmids. Lentiviral transfer vectors *HTT*Ex1-25Q, *HTT*Ex1-72Q and Sirt1, BDNF-luciferase construct (pIII(170)Luc)[6], Sirt1 and Sirt1 HY plasmids, Flag-CREB, TORC1, Flag-TORC1 and Flag-TORC1 S151A[7] were described previously. CREB, K-CREB, CREB-133 and pEGFP were purchased from Clontech. *HTT*Ex1 25Q-GFP, *HTT*Ex1-103Q-GFP, *HTT*480-17stop, *HTT*480-68stop, HA-TAF and CBP-HAT constructs were described previously [8]. Short hairpin RNA lentiviral plasmids (pLKO.1) targeting Sirt1 (5'-AAGTTGACCTCCTCATTGTTA-3') and TORC1 (5' TTGATTCAGACCATCAGTTTC-3') were purchased from Sigma. Lentiviral Sirt1 HY was generated by mutating 363 Histidine to Tyrosine.

Antibodies. Primary antibodies listed next were from the following sources: neurofilament (2H3, Developmental Studies Hybridoma Bank), Flag (F7425, Sigma), Flag M2 (F3165, Sigma), HA (HA.11, Covance, #3724, Cell Signaling), TORC1 (#2587, Cell Signaling Technology, #6937 from M. Montminy), phospho S151 TORC1 (#3359, Cell Signaling Technology), Myc (#2276, Cell Signaling Technology, sc-789, Santa Cruz, MCA1929, serotec), acetyl lysine (ICP0380, Immunechem), Sirt1 (07-131, Upstate, sc-15404, Santa Cruz, #2028, Cell Signaling and custom-made Sirt1 antibody from L. Guarente), β-tubulin (T4026, Sigma), β3-tubulin (#4466, Cell Signaling Technology), *HTT* (MAB5492 and MAB2166, Millipore, Ab1 from M. Difiglia), GFAP (#3670, Cell Signaling Technology), CREB (#9197, Cell Signaling Technology), phospho S133 CREB (06-519, Upstate) and α-tubulin (T5168, Sigma).

Primary neurons. Rat and mouse embryonic primary cortical neurons prepared from E19 and E17 embryos, respectively, were infected with lentiviral vectors at moi of 3 on DIV4. Lentivirus was produced as previously described[9]. Virus titer was determined using HIV-1 p24 Antigen ELISA kit (Zeptometrix). At 9 to 11 days post infection (dpi), neurons were fixed and stained with antibody to neurofilament. At least 20 fields per sample were randomly taken and staining intensity analyzed with ImageJ to assess mutant *HTT*-mediated toxicity. For in-cell western (ICW), neurons were plated in replicate in 96-well plates. Neurons fixed and double stained with antibody to neurofilament and Draq5 + Sapphire700 were analyzed using Odyssey Infrared Imaging System (LI-COR). Sirt1 KO and WT cultures were prepared by dissecting and plating each embryo separately from E16 littermates. Genotype of each embryo was determined after plating. BDNF was added to Sirt1 KO culture at 50 ng ml^{-1} every other day starting DIV5. Neurons were fixed at DIV14 for ICW. For knockdown of Sirt1, neurons were infected with sh scramble or sh Sirt1 lentivirus at moi of 1 on DIV8. At 5 days post infection (DIV13), neurons were treated with 25 μM forskolin (FSK) for indicated periods of time and probed for phospho TORC1 and total TORC1. For immunostaining of TORC1 after *HTT* expression, WT or mutant *HTT* lentivirus were infected at moi of 3 on DIV4 and neurons fixed and stained 6–7 days post infection. To determine if Sirt1

rescue of mutant *HTT* toxicity is dependent on TORC1 or CREB, *HTT*- and Sirt1-expressing lentivirus were infected at the same time at 3 moi on DIV4. sh TORC1, sh CREB or control virus were subsequently infected on DIV7. Neurons were fixed on DIV13 for NF staining.

Luciferase reporter assays and coimmunoprecipitations. Neuro2a (N2a) cells cultured in DMEM with 10% FBS were transfected using Lipofectamine 2,000. Tranfected cell were harvested at 24 h post transfection unless otherwise specified. For coimmunoprecipitation, transfected Neuro2a cells were harvested at 24 hr posttransfection and coimmunoprecipitation performed as previously described[10]. For luciferase reporter assays, Neuro2a cells were plated in 24-well plates in triplicate. The total DNA amount was kept constant by addition of empty vectors. 50 ng of reporter was used per well of 24-well plates. Cell extracts were prepared at 24 to 48 hr posttransfection and luciferase assay performed by standard protocol.
For alkaline phosphatase treatment**,** Neuro2a cells co-transfected with Flag-CREB and TORC1 was immunoprecipitated with antibody to flag. Dephosphorylation reactions were carried out on coimmunoprecipitated TORC1-containing protein G beads at 37ºC for 30 min with 40 units calf intestinal alkaline phosphatase (NEB) in 50 mM Tris (pH 7.9), 100 mM NaCl, 10 mM $MgCl_2$, 1 mM DTT and 100 μg ml^{-1} BSA.

Multidimensional Protein Identification Technology (MudPIT) and LTQ Orbitrap Mass Spectromtery. The precipitate was resuspended in 8 M Urea with ProteasMAX (Promega) per the manufacturer's instruction. The samples were subsequently reduced by 20 minute incubation with 5mM TCEP (*tris* 2 carboxyethyl phosphine) at room temperature and alkylated in the dark by treatment with 10 mM Iodoacetamide for 20 additional minutes. The proteins were digested overnight at 37 ºC with Sequencing Grade Modified Trypsin (Promega) and the reaction was stopped by acidification. The protein digest was pressure-loaded onto a 250--μm i.d capillary packed with 2.5 cm of 10-μm Jupiter C18 resin (Phenomenex) followed by an additional 2.5 cm of 5-μm Partisphere strong cation exchanger (Whatman). The column was washed with buffer containing 95% water, 5% acetonitrile, and 0.1% formic acid. After washing, a 100--μm i.d capillary with a 5-μm pulled tip packed with 15 cm 4-μm Jupiter C18 resin (Phenomenex) was attached to the filter union and the entire split-column (desalting column–filter union–analytical column) was placed inline with an Agilent 1200 quaternary HPLC (Agilent) and analyzed using a modified 5-step separation described previously[11]. The buffer solutions used were 5% acetonitrile/0.1% formic acid (buffer A), 80% acetonitrile/0.1% formic acid (buffer B), and 500 mM ammonium acetate/5% acetonitrile/0.1% formic acid (buffer C). Step 1 consisted of a 80 min gradient from 0–100% buffer B. Steps 2–4 had a similar profile except 5 min of 100% buffer A, 3 min of X% buffer C, a 10 min gradient from 0–15% buffer B, and a 108 min gradient from 15–100% buffer B. The 5 min buffer C percentages (X) were 40, 70, 100% respectively for the 4-step analysis. As peptides eluted from the microcapillary column, they were electrosprayed directly into an *LTQ Orbitrap* XL mass spectrometer (Thermo Finnigan) with the application of a distal 2.4 kV spray voltage. A cycle of one full-scan mass spectrum (400–1600 m/z) followed by 5

data dependent MS/MS spectra at a 35% normalized collision energy was repeated continuously throughout each step of the multidimensional separation. Application of mass spectrometer scan functions and HPLC solvent gradients were controlled by the Xcaliber data system.

Analysis of Tandem Mass Spectra. MS/MS spectra were analyzed using the following software analysis protocol. Poor quality spectra were removed from the dataset using an automated spectral quality assessment algorithm[12]. MS/MS spectra remaining after filtering were searched with the ProLuCID algorithm against the EBI-IPI_Human_3_30_06-28-2007 concatenated to a decoy database in which the sequence for each entry in the original database was reversed[13]. All searches were parallelized and performed on a Beowulf computer cluster consisting of 100 1.2GHz Athlon CPUs[14]. Searches were performed with Cystein carbamidomethylation as a fixed modification and Lysine acetylation was searched as a differential modification with an additional mass of 42.01056 Da. ProLuCID[15] results were assembled and filtered using the DTASelect (version 2.0) program[16]. DTASelect 2.0 uses a linear discriminate analysis to dynamically set XCorr and DeltaCN thresholds for the entire dataset to achieve a user-specified false positive rate (5% in this analysis). The false positive rates are estimated by the program from the number and quality of spectral matches to the decoy database. Confidence for modifications was estimated from overlapping modified peptides as described previously[17]. Only peptides with at least 1 tryptic termini were considered. The validity of peptide/spectrum matches was assessed using the SEQUEST-defined parameters, cross-correlation score (XCorr), and normalized difference in cross-correlation scores (DeltaCn).

Chromatin immunoprecipitation assays. Chromatin immunoprecipitation (ChIP) assay from mouse brains was performed using Magna ChIP kit (Millipore) according to manufacturer's protocol by using TORC1 antibody (#6937, PBL-Salk Institute) and normal rabbit IgG (Santa Cruz). The primer sequences for BDNF promoter IV were published previously[18].

Site-directed mutagenesis of TORC1. TORC1 mutants were generated by using QuikChange II XL site-directed mutagenesis kit (Agilent). Incorporation of mutations was verified by DNA sequencing (MGH DNA sequencing core).

Microarray analysis. mRNA was isolated from the striatum of 70 day old mice of the indicated genotypes using Trizol (Invitrogen). Microarray hybridization was performed by the NIH Neuroscience Microarray Consortium using Illumina gene chips. Data were analyzed using Gene Set Enrichment Analysis [2].

References for Supplementary Information

1. Bordone, L.*, et al.* SIRT1 transgenic mice show phenotypes resembling calorie restriction. *Aging cell* **6**, 759-767 (2007).
2. Subramanian, A.*, et al.* Gene set enrichment analysis: a knowledge-based approach for interpreting genome-wide expression profiles. *Proceedings of the National Academy of Sciences of the United States of America* **102**, 15545-15550 (2005).
3. Cui, L.*, et al.* Transcriptional repression of PGC-1alpha by mutant huntingtin leads to mitochondrial dysfunction and neurodegeneration. *Cell* **127**, 59-69 (2006).
4. Stack, E.C.*, et al.* Chronology of behavioral symptoms and neuropathological sequela in R6/2 Huntington's disease transgenic mice. *The Journal of comparative neurology* **490**, 354-370 (2005).
5. Spandidos, A., Wang, X., Wang, H. & Seed, B. PrimerBank: a resource of human and mouse PCR primer pairs for gene expression detection and quantification. *Nucleic acids research* **38**, D792-799.
6. Tao, X., Finkbeiner, S., Arnold, D.B., Shaywitz, A.J. & Greenberg, M.E. Ca2+ influx regulates BDNF transcription by a CREB family transcription factor-dependent mechanism. *Neuron* **20**, 709-726 (1998).
7. Conkright, M.D.*, et al.* TORCs: transducers of regulated CREB activity. *Molecular cell* **12**, 413-423 (2003).
8. Jeong, H.*, et al.* Acetylation targets mutant huntingtin to autophagosomes for degradation. *Cell* **137**, 60-72 (2009).
9. Tiscornia, G., Singer, O. & Verma, I.M. Production and purification of lentiviral vectors. *Nature protocols* **1**, 241-245 (2006).
10. Sarbassov, D.D.*, et al.* Rictor, a novel binding partner of mTOR, defines a rapamycin-insensitive and raptor-independent pathway that regulates the cytoskeleton. *Curr Biol* **14**, 1296-1302 (2004).
11. Washburn, M.P., Wolters, D. & Yates, J.R., 3rd. Large-scale analysis of the yeast proteome by multidimensional protein identification technology. *Nature biotechnology* **19**, 242-247 (2001).
12. Bern, M., Goldberg, D., McDonald, W.H. & Yates, J.R., 3rd. Automatic quality assessment of peptide tandem mass spectra. *Bioinformatics (Oxford, England)* **20 Suppl 1**, i49-54 (2004).
13. Peng, J., Elias, J.E., Thoreen, C.C., Licklider, L.J. & Gygi, S.P. Evaluation of multidimensional chromatography coupled with tandem mass spectrometry (LC/LC-MS/MS) for large-scale protein analysis: the yeast proteome. *Journal of proteome research* **2**, 43-50 (2003).
14. Sadygov, R.G.*, et al.* Code developments to improve the efficiency of automated MS/MS spectra interpretation. *Journal of proteome research* **1**, 211-215 (2002).
15. Yates, J.R., 3rd, Eng, J.K., McCormack, A.L. & Schieltz, D. Method to correlate tandem mass spectra of modified peptides to amino acid sequences in the protein database. *Analytical chemistry* **67**, 1426-1436 (1995).

16. Tabb, D.L., McDonald, W.H. & Yates, J.R., 3rd. DTASelect and Contrast: tools for assembling and comparing protein identifications from shotgun proteomics. *Journal of proteome research* **1**, 21-26 (2002).
17. MacCoss, M.J., Wu, C.C. & Yates, J.R., 3rd. Probability-based validation of protein identifications using a modified SEQUEST algorithm. *Analytical chemistry* **74**, 5593-5599 (2002).
18. Gao, J.*, et al.* A novel pathway regulates memory and plasticity via SIRT1 and miR-134. *Nature* **466**, 1105-1109 (2010).